ISSN 0006-2979, Biochemistry (Moscow), 2025, Vol. 90, No. 1, pp. 32-43 © Pleiades Publishing, Ltd., 2025.
Published in Russian in Biokhimiya, 2025, Vol. 90, No. 1, pp. 35-47.

MINI-REVIEW

A Portrait of Three Mammalian Bicistronic mRNA Transcripts, Derived from the Genes *ASNSD1*, *SLC35A4*, and *MIEF1*

Dmitry E. Andreev[1,2,a]* and Ivan N. Shatsky[2,b]

[1]*Shemyakin–Ovchinnikov Institute of Bioorganic Chemistry, Russian Academy of Sciences, 117997 Moscow, Russia*
[2]*Belozersky Institute of Physico-Chemical Biology, Lomonosov Moscow State University, 119992 Moscow, Russia*
[a]*e-mail: cycloheximide@yandex.ru* [b]*e-mail: ivanshatskyster@gmail.com*

Received October 4, 2024
Revised November 25, 2024
Accepted December 7, 2024

Abstract—Recent advances in functional genomics have allowed identification of thousands of translated short open reading frames (sORFs) in the 5′ leaders of mammalian mRNA transcripts. While most sORFs are unlikely to encode functional proteins, a small number have been shown to have evolved as protein-coding genes. As a result, dozens of these sORFs have already been annotated as protein-coding ORFs. mRNAs that contain both a protein-coding sORF and an annotated coding sequence (CDS) are referred to as bicistronic transcripts. In this study, we focus on three genes – *ASNSD1*, *SLC35A4*, and *MIEF1* – which give rise to bicistronic mRNAs. We discuss recent findings regarding functional investigation of the corresponding polypeptide products, as well as how their translation is regulated, and how this unusual genetic arrangement may have evolved.

DOI: 10.1134/S0006297924603630

Keywords: translation initiation, reinitiation, leaky scanning, dual coding, bicistronic mRNA

INTRODUCTION

Pioneering works by Marylin Kozak has allowed us to understand the basic mechanism of translation initiation in eukaryotic cells, which is based on the ribosomal scanning through the mRNA 5′-leader sequence [1]. According to this scanning model, the m^7G cap at the 5′-end of all mRNA molecules is first recognized by the eIF4F, which allows the 43S ribosomal complex recruitment on mRNA via the eIF4F-eIF3 interaction. The 43S complex then begins to scan the 5′-leader sequence in the 5′ to 3′ direction until the start codon (usually AUG) is recognized. This triggers detachment of the initiation factors, association with the 60S subunit, and allows elongation process to begin (see reviews [2-5]).

The mRNA 5′-leader sequences play an essential role in the scanning mechanism, as the obstacles along the path of the scanning ribosome complex decrease the number of ribosomes that successfully reach the AUG start codon of the main open reading frame. Interestingly, approximately half of the mammalian mRNAs contain at least one upstream AUG codon that creates an upstream reading frame (uORF) [6-10]. With the development of ribosome profiling, which allows detecting translating ribosomes with single-nucleotide resolution genome wide [11], it has been possible to demonstrate widespread translation events within the 5′-leaders, thus making the accepted terminology of 5′-untranslated regions (5′-UTRs) obsolete.

Functional roles of uORFs are under intense investigation. A growing number of studies have shown that some uORFs are involved in control of translation of the main open reading frame (ORF), but we will not focus on this aspect as it has been extensively covered in several recent reviews [4, 12-21]. In addition to their regulatory functions, some uORFs also encode functional polypeptides. Bicistronic mRNAs

Abbreviations: CDS, coding sequence; ISR, integrated stress response; sORF, short open reading frame; PFDL, prefoldin-like module; RNP, ribonucleoprotein particle; uORF, upstream open reading frame

* To whom correspondence should be addressed.

are a type of mRNAs that encode two proteins in two separate ORFs, and the ratio of these proteins can be regulated at the translation level. Here, we will discuss three examples of mammalian bicistronic mRNAs that have been extensively studied, and speculate how their translation can be regulated. We will also propose how changing the ratio of the two polypeptides for these selected cases can affect cell physiology.

ASDURF-ASNSD1

The *ASNSD1* gene locus encodes a poorly characterized protein that is predicted to have asparagine synthase (glutamine-hydrolyzing) activity. Additionally, there is a short protein coding gene called *ASDURF* (ENSG00000286053), which is either expressed as a separate ORF due to utilization of an alternative polyadenylation site located in exon 4 (within the *ASNSD1* CDS [coding sequence]), or as an upstream ORF in an alternative transcript. According to the cap analysis of gene expression (CAGE) data from the FANTOM5 project [22] (visualized in the Zenbu browser [23]), these two genes share a single promoter. Therefore, *ASNSD1* could only be translated from the same mRNA, which also contains the upstream *ASDURF* (Fig. 1a, Fig. S1A in the Online Resource 1).

ASDURF (a.k.a. ASNSD1-SEP) was initially identified by Slavoff et al. [24] by using peptidomics approach optimized for identification of the short ORF-encoded peptides. Using isotope dilution mass spectrometry [25], it was demonstrated that the intracellular concentration of ASDURF in K562 cells was 386 molecules per cell [24]. The function of ASDURF remained enigmatic until 2020, when Cloutier et al. provided compelling evidence that it was a subunit of the prefoldin-like module (PFDL) of PAQosome [26]. The PAQosome or Rvb1–Rvb2–Tah1–Pih1/prefoldin-like (R2TP/PFDL) complex is a specific chaperone complex responsible for assembly and maturation of many key multiprotein complexes in mammalian cells [27]. In mammals, this complex consists of two modules, R2TP and PFDL. Cloutier et al. first implemented the proximity-dependent biotinylation (BioID) to identify new interacting proteins with two known PAQosome subunits, PIH1D1 and UXT, and found that the endogenous ASDURF was highly enriched in both experiments. Next, the FLAG-based affinity purification mass spectrometry (AP-MS) was also performed on two additional PAQosome subunits, RPAP3 and URI1. Again, ASDURF was among the highly enriched interacting proteins. Furthermore, the FLAG-based purification of ASDURF revealed subunits of the PAQosome, confirming that ASDURF is an integral component of the PFDL module. *In vitro* assembly of the PFDL complex from the purified components showed that ASDURF is the 6th subunit of PFDL heterohexamer complex, which also consists of UXT1, PFDN6, PDRG1, URI1, and PFDN2. Interaction of ASDURF with the PFDN subunits has also been independently confirmed by Hofman et al. [28].

PAQosome is involved in the activity of many multi-subunit protein and ribonucleoprotein particle (RNP) complexes such as ribonucleoproteins of the L7Ae family (box C/D and H/ACA snoRNPs, U4 snRNPs, and telomerase and selenoprotein mRNPs), U5 snRNP, phosphatidylinositol 3-kinase-related kinase complexes (PIKKs) (ATM, ATR, DNA-PKcs, mTOR, SMG-1, and TRRAP), and RNA polymerases I, II, and III [33-38]. If ASDURF is essential for the PAQosome function, its absence could affect cell fate. Recently, using the CRISPR-Cas9 screens, Hofman et al. [28] demonstrated that targeting *ASDURF* decreases cell viability in the MYC-driven medulloblastoma cell lines. Importantly, re-expression of *ASDURF* rescues this phenotype. *In vivo*, the knockout of *ASDURF* prolonged the overall survival of mice with orthotopic xenografts of the D425 MYC-driven medulloblastoma cells. Interestingly, the *ASDURF* knockout *in vitro* reduced S-phase incorporation of bromouridine, suggesting that ASDURF/PFDL activity could be involved in the cell cycle control in the MYC-driven medulloblastoma. Less is known about the *ASNSD1*, which is encoded by the second cistron. ASNSD1 has an N-terminal class-II glutamine amidotransferase domain and a C-terminal asparagine synthase B domain belonging to the adenine nucleotide alpha hydrolase (AANH) superfamily, and it is likely involved in asparagine synthesis.

Analysis of the aggregated riboseq datasets from human cells reveals three translated regions: a short uORF encoding the MP dipeptide located 46 nts upstream of the first cistron, the *ASDURF* (first cistron), and the *ASNSD1* (second cistron) (Fig. 1b). Triplet periodicity of the riboseq signal is consistent with translation of these reading frames. The *ASDURF* gene is translated by one order of magnitude more efficiently than the *ASNSD1*, which, likely, indicates that translation of the first cistron strongly repress translation of the second cistron (Fig. 1b). Interestingly, however, in the experiments with reporter constructs mutation of the *ASDURF* start codon derepresses translation of the luciferase fused to the second cistron only ~2 fold [39], which is less than expected. This suggests that when the AUG of *ASDURF* is mutated, the ribosomes begin to initiate translation at the AUG codons within the *ASDURF* reading frame that are normally not recognized, when the *ASDURF* start site is active.

Phylogenetic analysis reveals that the sequence of *ASDURF* corresponding to the 1st exon is conserved in mammals, while the 2nd and 3rd exons show high rate of synonymous codon substitutions also across the vertebrate genomes (Fig. 1c).

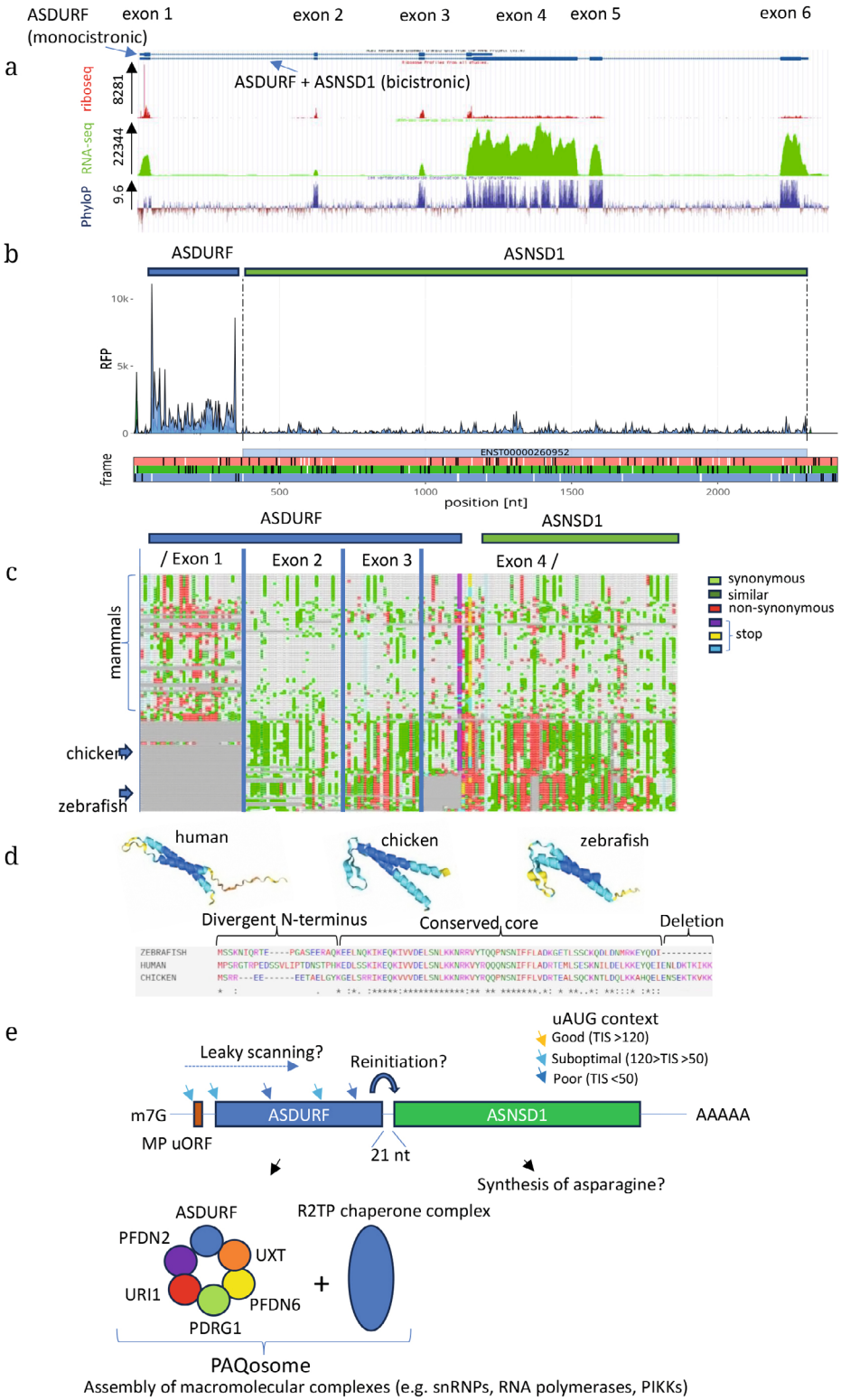

Fig. 1. a) Aggregated Riboseq and RNAseq data for the *ASNSD1* gene from the GWIPS-Viz browser [29]. Nucleotide evolutionary conservation is shown as 100 vertebrates Basewise Conservation by PhyloP (phyloP100way) track [30]. b) Aggregated Riboseq data from the Ribocrypt transcriptome browser (ribocrypt.org, in preparation), ribosome footprints are color-coded according to the translated reading frames shown below in the diagram. c) Multiple sequence alignment performed with CodAlignView ("CodAlignView: A tool for Exploring Signatures of Protein-Coding Evolution in an Alignment", Jungreis, I., Lin, M., and Kellis, M., in preparation), the alignment set used was hg30_100. d) Structures and alignment of human, chicken, and zebrafish ASDURF. Structures were generated using AlphaFold 3 [31]. Sequence alignment was performed with ClustalW [32]. e) Schematic representation of the *ASDURF-ASNSD1* bicistronic mRNA. AUG codons upstream of the second cistron are marked with colored arrows. The proposed functions of proteins encoded in cistrons are presented below.

Analysis of the chicken and zebrafish *ASNSD1* genes shows that these organisms use alternative first exons, which contain an in-frame AUG codon. Due to this, the N-terminal portion of ASDUSF is variable. However, according to the AlphaFold 3 modelling, these proteins may have a similar structural organization consistent with the b-prefoldin structure (Fig. 1d).

How can translation of the *ASDURF-ASNSD1* bicistronic mRNA be regulated? To investigate efficiency of AUG codons, we explored the data from the quantitative analysis of mammalian translation, where the strength of AUG contexts from −6 to +5 positions was experimentally measured and quantified [40]. The AUG contexts efficiency ranges from 12 (least efficient) to 150 (most efficient). Interestingly, all the AUGs upstream of the *ASNSD1* CDS including the AUG of the *ASDURF* have suboptimal or weak contexts (Fig. 1e). Based on this information, we hypothesize that the *ASNSD1* translation may be regulated under conditions of altered stringency of start codon selection, or when the translation elongation rate is regulated. Increasing initiation at suboptimal AUG codons or slowing down the elongating ribosome that translates *ASDURF* is expected to significantly reduce the downstream translation of *ASNSD1*.

SLC35A4URF-SLC35A4

The *SLC35A4* gene locus encodes a protein that was initially predicted to have a pyrimidine nucleotide-sugar transmembrane transport activity. In addition, there is a short protein-coding gene ENSG00000293600 located upstream of the *SLC35A4* CDS. In parallel with other cases described here, we suggest calling this upstream open reading frame *SLC35A4URF*. *SLC35A4URF* could be translated either as a separate ORF, due to the use of alternative polyadenylation site between *SLC35A4* and *SLC35A4URF*, or as a bicistronic mRNA. Based on the cap analysis of gene expression (CAGE) data from the FANTOM5 project [22] (visualized in the Zenbu browser [23]), it appears that *SLC35A4* could only be translated from the bicistronic transcripts (Fig. 2a, Fig. S1B in the Online Resource 1).

In 2015, we predicted that the upstream open reading frame in the *SLC35A4* gene could encode a functional protein [41]. Functional role of SLC35A4URF or SLC35A4-MP has been the subject of two recent studies, and it has been shown that it plays a role in mitochondria [42, 43]. Yang et al. [43] demonstrated that the SLC35A4URF protein is localized in mitochondria. Using co-immunoprecipitation mass spectrometry (co-IP/MS) and Western blotting, they demonstrated that the SLC35A4URF interacts with the mitochondrial outer membrane proteins, such as VDAC1 and VDAC3. Additionally, co-immunostaining experiments revealed that the SLC35A4URF was colocalized with the outer membrane marker TOMM20. Rocha et al. [42] developed rabbit polyclonal antibodies against SLC35A4URF and demonstrated that the endogenous protein is located in mitochondria. However, based on the proteinase K assays, SLC35A4ORF appears to be a mitochondrial inner membrane protein rather than an outer membrane protein. These results are consistent with the presence of a single-pass transmembrane domain between the amino acids 62 and 84 of SLC35A4URF [42].

Functional role of *SLC35A4URF* has been shown to be linked to mitochondrial respiration. Using genome editing, Rocha et al. generated the KO HEK293T cell lines and demonstrated that the loss of this protein resulted in significant decrease in basal proton leak and maximal respiration. Conversely, overexpression of the *SLC35A4URF* gene leads to the increase in maximal capacity rates. Interestingly, 3-fold overexpression of *SLC35A4URF* in the MCF7 cells impairs cell growth, which was accompanied by the loss of mitochondrial membrane potential and upregulation of transcription of the genes enriched in the mitochondria-related pathways such as “response to hypoxia” and “negative regulation of mitochondrial membrane potential”. This suggests that the amount of SLC35A4URF protein must be tightly regulated in order to promote optimal cellular growth.

Function of the second cistron product, SLC35A4, is related to regulation of glycosylation in the Golgi apparatus. SLC35A4 and its paralog SLC35A1 could be involved in the transport of CDP-ribitol from the cytoplasm to Golgi [44]. CDP-ribitol, which is synthetized by the ISPD enzyme in the cytoplasm, is used for assembly of a complex glycan on the α-dystroglycan glycoprotein by the FKTN and FKRP enzymes in the Golgi apparatus [45]. Modification with the ribitol moieties is required for proper interaction of α-dystroglycan with extracellular matrix proteins such as laminin. Localization of the overexpressed SLC35A4 in the Golgi was experimentally confirmed by Rocha et al. [42].

The aggregated riboseq data for the human *SLC35A4URF-SLC35A4* mRNA reveals efficient translation of the first cistron and almost undetectable translation of the second cistron (Fig. 2, a and b). The first 312-nt-long ORF is followed by the long spacer region of 407 nucleotides that contains several AUG codons (11 in total preceding the second cistron). Phylogenetic analysis reveals that this spacer region is the least conserved in the vertebrate genomes (Fig. 2d). Interestingly, the riboseq data from zebrafish, where the spacer region is much shorter, reveals translation of both cistrons (Fig. 2c).

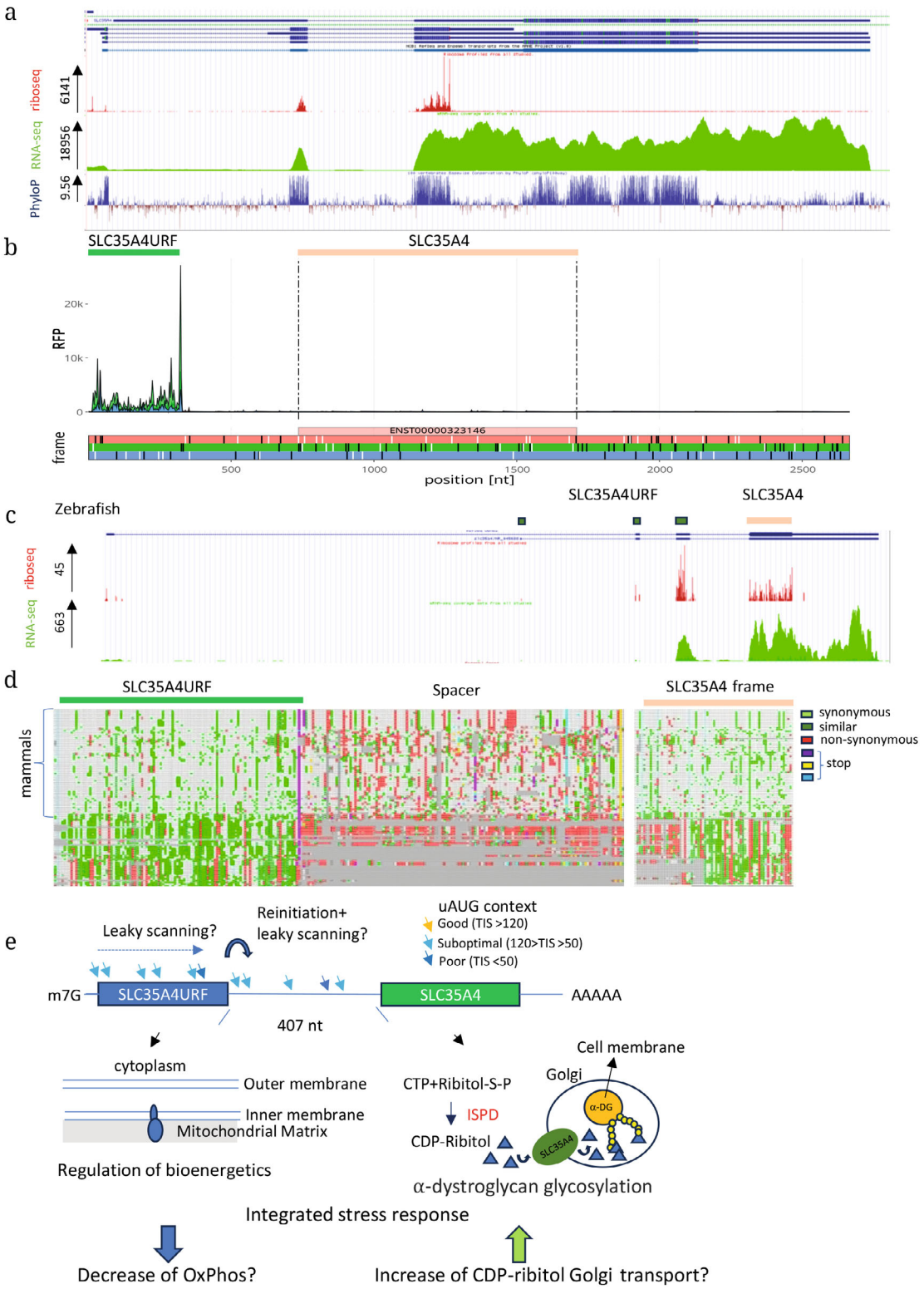

Fig. 2. a) Aggregated Riboseq and RNA-seq data for the *SLC35A4* gene from the GWIPS-Viz browser [29]. Nucleotide evolutionary conservation is displayed as 100 vertebrates Basewise Conservation by PhyloP (phyloP100way) track [30]. b) Aggregated Riboseq data from the Ribocrypt transcriptome browser (ribocrypt.org, in preparation). Ribosome footprints are color-coded according to the translated reading frames shown below in the diagram. c) Aggregated Riboseq and RNAseq data for the zebrafish *SLC35A4* gene from the GWIPS-Viz browser [29]. d) Multiple sequence alignment performed with CodAlignView ("CodAlignView: A tool for Exploring Signatures of Protein-Coding Evolution in an Alignment", Jungreis, I., Lin, M., and Kellis, M., in preparation), the alignment set used is hg30_100. e) Schematic representation of the *SLC35A4URF-SLC35A4* bicistronic mRNA. AUG codons located upstream of the second cistron are marked with colored arrows. Possible functions for the proteins encoded in both cistrons are shown below.

Regulation of translation of the *SLC35A4URF-SLC35A4* bicistronic mRNA during the integrated stress response has been discovered in two independent studies [41, 46]. During the integrated stress response (ISR), translation of the *SLC35A4* increases significantly, which is accompanied by downregulation of the first cistron. Andreev et al. [41] performed a reporter analysis with the reporter mRNA, where the second cistron has been replaced with firefly luciferase. Under normal conditions, this capped bicistronic mRNA produced very low but detectable levels of reporter activity, which was approximately two orders of magnitude lower than that for the reporter mRNA with the short 5′-leader. After treatment with arsenite, which activates eIF2 phosphorylation, translation of the second cistron increased, while translation of the control mRNA decreased approximately 10-fold. Therefore, the sequence upstream of the *SLC35A4* second cistron appears to be sufficient to mediate stress resistant translation. Sequence analysis reveals that all 11 AUG codons upstream of the second cistron contain non-optimal nucleotide contexts (Fig. 2e), which raises the possibility that translation of the second cistron could be mediated by leaky scanning.

Taken together, translation control of *SLC35A4URF-SLC335A4* could connect mitochondrial respiration with extracellular matrix. During the integrated stress response, translation of the first cistron is decreased, which apparently should lead to the decrease in mitochondrial respiration. At the same time, the stress-induced activation of translation of *SLC35A4* could support maturation of α-dystroglycan. It is worth noting that the *SLC35A1* translation, which is also involved in the CDP-ribitol transport, is significantly downregulated during the arsenite-induced stress [41]. Interestingly, when *SLC35A4* is overexpressed in the cells lacking *SLC35A1*, glycosylation of α-dystroglycan is rescued, but molecular weight of the glycosylated form of α-dystroglycan is significantly decreased [44]. This indicates that SLC35A4 could alter glycosylation pattern of its substrate. This allows us to speculate that under stress conditions, the α-dystroglycan glycosylation pattern could be altered due to the changes in the ratio of SLC35A4 to SLC35A1.

MIURF-MIEF1

The *MIEF1* gene locus was suggested to encode a bicistronic mRNA based on phylogenetic analysis of its upstream uORF [41]. The product of the second cistron, MIEF1 protein, plays a role in regulating mitochondrial fusion and fission. Additionally, there is a micropeptide called MIURF encoded in the first cistron (ENSG00000285025) that operates in mitochondria and, likely, also regulates MIEF1. According to the cap analysis of gene expression (CAGE) data from the FANTOM5 project [22] (visualized in the Zenbu browser [23]), both *MIURF* and *MIEF1* share a common promoter (Fig. S1C in the Online Resource 1).

MIEF1 (a.k.a. MID51) and MIEF2 (a.k.a. MID49) are two closely related proteins that were discovered in 2011. These proteins are involved in regulation of mitochondrial dynamics, as they can change morphology of mitochondria (fission and fusion), when they are overexpressed or knocked out [47]. MIEFs are outer mitochondrial membrane proteins, which contain a single-pass transmembrane domain at the N-terminus with bulk of the protein facing the cytosol. MIEFs act as a receptor hub that recruits both pro-fusion proteins MFN1 and MFN2, and pro-fission protein DRP1 [48]. It was shown that MIEFs can form oligomers and self-associate, which could promote fusion of the adjacent mitochondria [48].

MIURF, a protein encoded in the first cistron, appears to have two mutually exclusive functions: regulation of mitochondrial translation, which takes place in the mitochondrial matrix, and regulation of MIEF1 activity on the cytoplasmic side of the mitochondrial outer membrane. Initially, MIURF was discovered as a component of the mitochondrial ribosome assembly intermediate for the large ribosomal subunit, LSU. Mitoribosomal assembly intermediates were isolated from the human cell line derived from HEK293S cells and analyzed using cryo-EM. The authors observed a density adjacent to uL14m and used the density-based fold-recognition pipeline and mass-spectrometry analysis to identify three proteins: MALSU, mt-ACP, and MIURF (known as L0R8F8 at the time of publication). This module was proposed to prevent premature association of the ribosomal subunits [49]. Rathore et al. [50] supported the role of MIURF in the regulation of mitochondrial translation. Using various approaches, the authors demonstrated that MIURF interacts with the mitochondrial ribosome and that MIURF positively regulates mitochondrial translation. In both studies mitochondrial ribosomes were shown to interact with the endogenous MIURF, which strongly supports its functional role in translation. Whether MIURF serves exclusively as a mitoribosome assembly factor, or is it also a component of the mature translation machinery, remains to be determined.

Another activity of MIURF was discovered in 2020. Chen et al. [51] performed genome-wide CRISPR screening to identify non-canonical CDSs that influence cellular growth; and this approach allowed them to identify MIURF as one of the top hits. They further showed that the overexpressed tagged MIURF physically interacts with the second cistron product, MIEF1. Importantly, the tagged MIEF1 pulls down MIURF. Interestingly, overexpression of *MIURF* induces

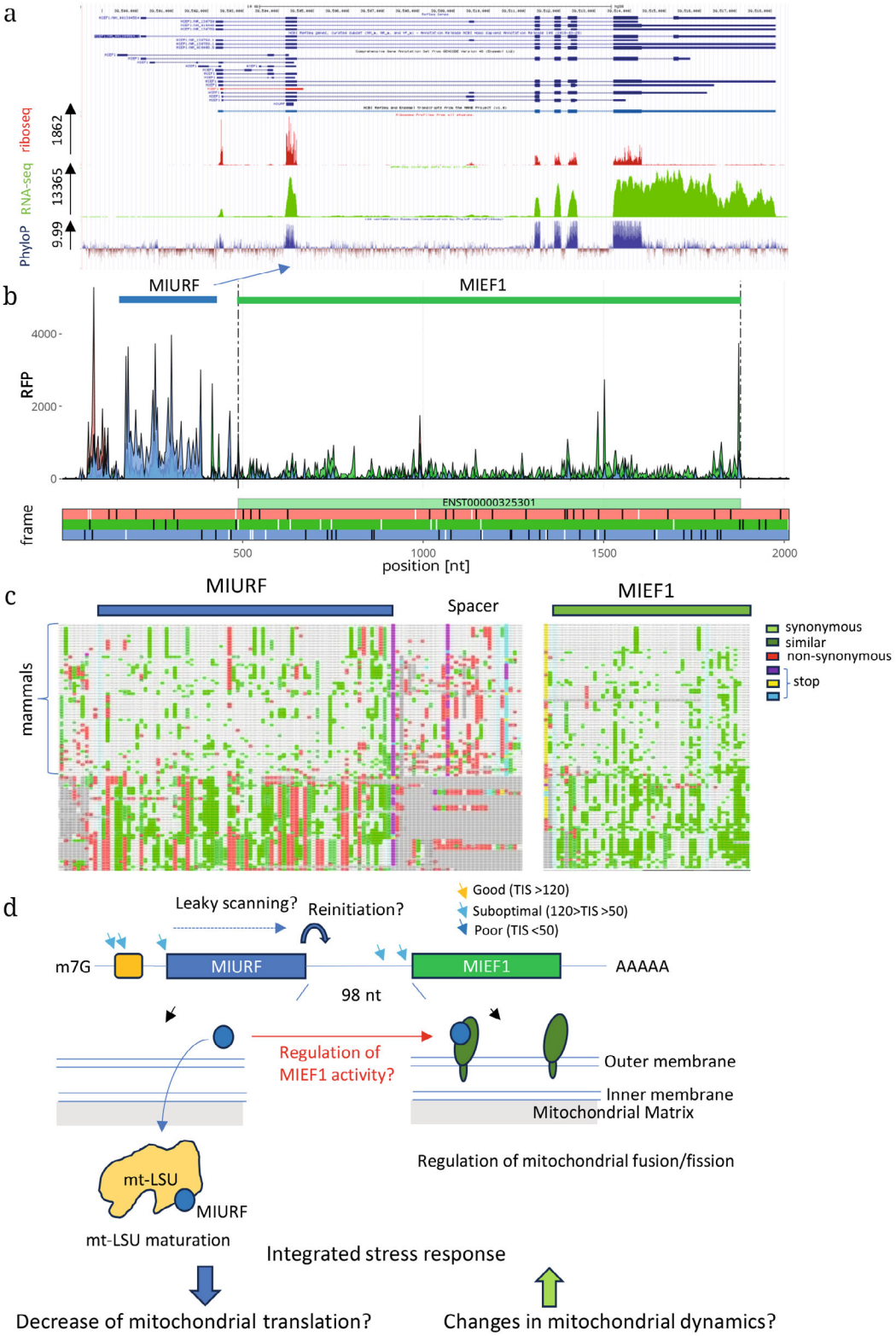

Fig. 3. a) Aggregated Riboseq and RNAseq data for the MIEF1 gene from the GWIPS-Viz browser [29]. Nucleotide evolutionary conservation is shown as the 100 vertebrates Basewise Conservation by PhyloP (phyloP100way) track [30]. b) Aggregated Riboseq data from the Ribocrypt transcriptome browser (ribocrypt.org, in preparation). Ribosome footprints are color-coded according to the translated reading frames shown below the diagram. c) Multiple sequence alignment performed with CodAlignView ("CodAlignView: A tool for Exploring Signatures of Protein-Coding Evolution in an Alignment", Jungreis, I., Lin, M., and Kellis, M., in preparation), the alignment set used is hg30_100. d) Schematic representation of the *MIURF-MIEF1* bicistronic mRNA. AUG codons located upstream of the second cistron are marked with colored arrows. Possible functions for the proteins encoded in both cistrons are shown below.

a fragmented mitochondrial phenotype (increased fission), while knockout of *MIURF* results in increased fusion, which can be rescued by exogenous expression of *MIURF*. These findings suggest that MIURF could influence activity of MIEF1 by modulating its interaction with the fusion/fission machinery on the cytosolic side of the mitochondrial outer membrane.

To understand how *MUIRF-MIEF1* translation can be regulated, we analyzed riboseq data (Fig. 3, a and b) and performed phylogenetic analysis (Fig. 3c). The aggregated Riboseq data supports translation of both cistrons from the bicistronic mRNA. In humans, bisictronic mRNA contains five AUG codons upstream of the *MIEF1* CDS. The 3rd AUG in a suboptimal nucleotide context initiates translation of the *MIURF* coding sequence. Analysis of the vertebrate genomes reveals that the *MIURF* reading frame is conserved among vertebrates, and the spacer region between *MIURF* and *MIEF1* is less conserved. All five upstream AUG codons are in suboptimal contexts, raising the possibility that translation of the second cistron could be regulated by leaky scanning (Fig. 3d).

Interestingly, translation of *MIURF* and *MIEF1* has been shown to be differentially regulated under the ISR induced by arsenite treatment [41]. The ISR conditions have significantly decreased the ratio of *MIURF* to *MIEF1* translation. This finding suggests that the ISR-mediated translation control of *MIURF* and *MIEF1* could influence various mitochondrial activities. Under normal conditions, *MIURF* is produced at higher levels than *MIEF1*. Proteomic analysis performed in [52] revealed that the ratio of MIURF/MIEF proteins under normal growth conditions in the HEK 293, HeLa, and human colon tissue cells is 2.71, 5.73, and 2.62, respectively. As MIURF is synthesized in the cytosol, it has an opportunity to bind immediately to MIEF1, which is localized on the outer mitochondrial membrane (OMM). Excess of MIURF is expected to be transported to the mitochondrial matrix for mitochondrial ribosome biogenesis. Under stress conditions, the ratio of MIURF to MIEF1 decreases. If all MIURFs become trapped in the complexes with MIEF1, mitochondrial ribosomal biogenesis would be blocked. However, this hypothetical mechanism requires experimental verification.

DISCUSSION

Here, we present analysis of the recent data on translational regulation and function of three bicistronic messenger RNAs that are evolutionarily conserved in vertebrates. Interestingly, all three cases show that the two cistrons play distinct functional roles. This raises the question of how these bisictronic genes evolved. Notably, all three genes have paralogous second cistron genes (*ASNS*, *SLC35A1*, *A2*, *A3*, *A5*, and *MIEF2*) that do not contain corresponding uORFs. This suggests that *ASNSD1*, *SLC35A4*, and *MIEF1* may have originated from the gene duplication events followed by fusion to the first cistron, which initially operated as an individual gene. These fusions created the translationally controlled regulatory circuits that benefitted organism fitness and were fixed in evolution. Interestingly, the intercistronic sequences that are expected to regulate translation, are less conserved than the cistrons themselves. This implies that these sequences have evolved differently to adjust translational control. This can be illustrated by the *SLC35A4* gene in humans, which has a much longer spacer and contains more AUG codons compared to the zebrafish gene (5 vs. 1 AUG).

Unusual bicistronic organization suggests that two cistrons are under translation control. Changes in activity of the translation machinery can quickly alter the ratio of polypeptides encoded in the upstream and downstream open reading frames. Indeed, two out of three mRNAs described here showed these changes during the integrated stress response, when the eIF2-tRNAi-GTP (TC) concentration becomes limited. It is highly likely that translation regulation of these mRNAs is not limited to the integrated stress response. We noticed that in all three cases, AUG initiation codons located upstream of the second cistron have non-optimal nucleotide contexts, raising the possibility of regulation through alterations in the start codon selection stringency. Key players in this process are eIF1 and eIF5 [53-59]. Increased levels of eIF1 decrease initiation at suboptimal codons, while eIF5 has the opposite effect. We assume that these factors would significantly influence translation of the bicistronic mRNAs described in this study. Another potential regulator of bicistronic mRNA translation is eIF4G2, also known as DAP5. Several recent studies have shown that eIF4G2 regulates translation of the uORF-containing mRNAs by either promoting reinitiation or leaky scanning [60-65]. In particular, eIF4G2 has been shown to regulate translation of the dual-coding *POLG* mRNA, where initiation at the highly efficient CUG codon allows translation of the POLGARF protein [66]. It would be extremely interesting to identify the factors that could change the ratio of translation of the two cistrons for *ASNSD1*, *SLC35A4*, and *MIEF1*.

The number of annotated bicistronic mRNAs continue to increase. For instance, 25 uORFs were recently annotated as new protein coding genes [67]. Functional investigation of these uORF-encoded proteins would help us to better understand genome evolution and the coupling of various cellular processes mediated by the translation control of bicistronic mRNAs. This is exemplified by the cases of *ASNSD1*, *SLC35A4*, and *MIEF1*, which are discussed in this paper.

Supplementary information. The online version contains supplementary material available at https://doi.org/10.1134/S0006297924603630.

Contributions. Dmitry E. Andreev conceived the study, analyzed the data, and wrote the manuscript; Dmitry E. Andreev and Ivan N. Shatsky edited the manuscript.

Funding. The work was supported by the Russian Science Foundation (project no. 20-14-00121).

Ethics approval and consent to participate. This work does not contain any studies involving human and animal subjects.

Conflict of interest. The authors of this work declare that they have no conflicts of interest.

REFERENCES

1. Kozak, M. (1980) Evaluation of the “scanning model” for initiation of protein synthesis in eucaryotes, *Cell*, **22**, 7-8, https://doi.org/10.1016/0092-8674(80)90148-8.
2. Hinnebusch, A. G. (2011) Molecular mechanism of scanning and start codon selection in eukaryotes, *Microbiol. Mol. Biol. Rev.*, **75**, 434-467, https://doi.org/10.1128/MMBR.00008-11.
3. Hinnebusch, A. G. (2014) The scanning mechanism of eukaryotic translation initiation, *Annu. Rev. Biochem.*, **83**, 779-812, https://doi.org/10.1146/annurev-biochem-060713-035802.
4. Hinnebusch, A. G., Ivanov, I. P., and Sonenberg, N. (2016) Translational control by 5′-untranslated regions of eukaryotic mRNAs, *Science*, **352**, 1413-1416, https://doi.org/10.1126/science.aad9868.
5. Shirokikh, N. E., and Preiss, T. (2018) Translation initiation by cap-dependent ribosome recruitment: Recent insights and open questions, *Wiley Interdiscip. Rev. RNA*, **9**, e1473, https://doi.org/10.1002/wrna.1473.
6. Rogozin, I. B., Kochetov, A. V., Kondrashov, F. A., Koonin, E. V., and Milanesi, L. (2001) Presence of ATG triplets in 5′ untranslated regions of eukaryotic cDNAs correlates with a ‘weak’ context of the start codon, *Bioinformatics*, **17**, 890-900, https://doi.org/10.1093/bioinformatics/17.10.890.
7. Suzuki, Y., Ishihara, D., Sasaki, M., Nakagawa, H., Hata, H., Tsunoda, T., Watanabe, M., Komatsu, T., Ota, T., Isogai, T., Suyama, A., and Sugano, S. (2000) Statistical analysis of the 5′ untranslated region of human mRNA using “Oligo-Capped” cDNA libraries, *Genomics*, **64**, 286-297, https://doi.org/10.1006/geno.2000.6076.
8. Pesole, G., Gissi, C., Grillo, G., Licciulli, F., Liuni, S., and Saccone, C. (2000) Analysis of oligonucleotide AUG start codon context in eukariotic mRNAs, *Gene*, **261**, 85-91, https://doi.org/10.1016/s0378-1119(00)00471-6.
9. Davuluri, R. V., Suzuki, Y., Sugano, S., and Zhang, M. Q. (2000) CART classification of human 5′ UTR sequences, *Genome Res.*, **10**, 1807-1816, https://doi.org/10.1101/gr.gr-1460r.
10. Andreev, D. E., Loughran, G., Fedorova, A. D., Mikhaylova, M. S., Shatsky, I. N., and Baranov, P. V. (2022) Non-AUG translation initiation in mammals, *Genome Biol.*, **23**, 111, https://doi.org/10.1186/s13059-022-02674-2.
11. Ingolia, N. T., Ghaemmaghami, S., Newman, J. R., and Weissman, J. S. (2009) Genome-wide analysis in vivo of translation with nucleotide resolution using ribosome profiling, *Science*, **324**, 218-223, https://doi.org/10.1126/science.1168978.
12. Dever, T. E., Ivanov, I. P., and Hinnebusch, A. G. (2023) Translational regulation by uORFs and start codon selection stringency, *Genes Dev.*, **37**, 474-489, https://doi.org/10.1101/gad.350752.123.
13. Tidu, A., and Martin, F. (2024) The interplay between cis- and trans-acting factors drives selective mRNA translation initiation in eukaryotes, *Biochimie*, **217**, 20-30, https://doi.org/10.1016/j.biochi.2023.09.017.
14. Renz, P. F., Valdivia-Francia, F., and Sendoel, A. (2020) Some like it translated: small ORFs in the 5′UTR, *Exp. Cell Res.*, **396**, 112229, https://doi.org/10.1016/j.yexcr.2020.112229.
15. Silva, J., Fernandes, R., and Romao, L. (2019) Translational regulation by upstream open reading frames and human diseases, *Adv. Exp. Med. Biol.*, **1157**, 99-116, https://doi.org/10.1007/978-3-030-19966-1_5.
16. Chen, H. H., and Tarn, W. Y. (2019) uORF-mediated translational control: recently elucidated mechanisms and implications in cancer, *RNA Biol.*, **16**, 1327-1338, https://doi.org/10.1080/15476286.2019.1632634.
17. Zhang, H., Wang, Y., and Lu, J. (2019) Function and evolution of upstream ORFs in eukaryotes, *Trends Biochem. Sci.*, **44**, 782-794, https://doi.org/10.1016/j.tibs.2019.03.002.
18. Cabrera-Quio, L. E., Herberg, S., and Pauli, A. (2016) Decoding sORF translation - from small proteins to gene regulation, *RNA Biol.*, **13**, 1051-1059, https://doi.org/10.1080/15476286.2016.1218589.
19. Young, S. K., and Wek, R. C. (2016) Upstream open reading frames differentially regulate gene-specific translation in the integrated stress response, *J. Biol. Chem.*, **291**, 16927-16935, https://doi.org/10.1074/jbc.R116.733899.
20. Wethmar, K. (2014) The regulatory potential of upstream open reading frames in eukaryotic gene expression, *Wiley Interdiscip. Rev. RNA*, **5**, 765-778, https://doi.org/10.1002/wrna.1245.
21. Somers, J., Poyry, T., and Willis, A. E. (2013) A perspective on mammalian upstream open reading frame function, *Int. J. Biochem. Cell Biol.*, **45**, 1690-1700, https://doi.org/10.1016/j.biocel.2013.04.020.
22. Lizio, M., Harshbarger, J., Shimoji, H., Severin, J., Kasukawa, T., Sahin, S., Abugessaisa, I., Fukuda, S., Hori, F., Ishikawa-Kato, S., Mungall, C. J., Arner, E.,

Baillie, J. K., Bertin, N., Bono, H., de Hoon, M., Diehl, A. D., Dimont, E., Freeman, T. C., Fujieda, K., Hide, W., Kaliyaperumal, R., Katayama, T., Lassmann, T., et al. (2015) Gateways to the FANTOM5 promoter level mammalian expression atlas, *Genome Biol.*, **16**, 22, https://doi.org/10.1186/s13059-014-0560-6.

23. Severin, J., Lizio, M., Harshbarger, J., Kawaji, H., Daub, C. O., Hayashizaki, Y., Consortium, F., Bertin, N., and Forrest, A. R. (2014) Interactive visualization and analysis of large-scale sequencing datasets using ZENBU, *Nat. Biotechnol.*, **32**, 217-219, https://doi.org/10.1038/nbt.2840.
24. Slavoff, S. A., Mitchell, A. J., Schwaid, A. G., Cabili, M. N., Ma, J., Levin, J. Z., Karger, A. D., Budnik, B. A., Rinn, J. L., and Saghatelian, A. (2013) Peptidomic discovery of short open reading frame-encoded peptides in human cells, *Nat. Chem. Biol.*, **9**, 59-64, https://doi.org/10.1038/nchembio.1120.
25. Keshishian, H., Addona, T., Burgess, M., Kuhn, E., and Carr, S. A. (2007) Quantitative, multiplexed assays for low abundance proteins in plasma by targeted mass spectrometry and stable isotope dilution, *Mol. Cell. Proteomics*, **6**, 2212-2229, https://doi.org/10.1074/mcp.M700354-MCP200.
26. Cloutier, P., Poitras, C., Faubert, D., Bouchard, A., Blanchette, M., Gauthier, M. S., and Coulombe, B. (2020) Upstream ORF-encoded ASDURF is a novel prefoldin-like subunit of the PAQosome, *J. Proteome Res.*, **19**, 18-27, https://doi.org/10.1021/acs.jproteome.9b00599.
27. Houry, W. A., Bertrand, E., and Coulombe, B. (2018) The PAQosome, an R2TP-based chaperone for quaternary structure formation, *Trends Biochem. Sci.*, **43**, 4-9, https://doi.org/10.1016/j.tibs.2017.11.001.
28. Hofman, D. A., Ruiz-Orera, J., Yannuzzi, I., Murugesan, R., Brown, A., Clauser, K. R., Condurat, A. L., van Dinter, J. T., Engels, S. A. G., Goodale, A., van der Lugt, J., Abid, T., Wang, L., Zhou, K. N., Vogelzang, J., Ligon, K. L., Phoenix, T. N., Roth, J. A., Root, D. E., Hubner, N., et al. (2024) Translation of non-canonical open reading frames as a cancer cell survival mechanism in childhood medulloblastoma, *Mol. Cell*, **84**, 261-276.e218, https://doi.org/10.1016/j.molcel.2023.12.003.
29. Michel, A. M., Fox, G., Kiran, A. M., De Bo, C., O'Connor, P. B., Heaphy, S. M., Mullan, J. P., Donohue, C. A., Higgins, D. G., and Baranov, P. V. (2014) GWIPS-viz: development of a ribo-seq genome browser, *Nucleic Acids Res.*, **42**, D859-D864, https://doi.org/10.1093/nar/gkt1035.
30. Pollard, K. S., Hubisz, M. J., Rosenbloom, K. R., and Siepel, A. (2010) Detection of nonneutral substitution rates on mammalian phylogenies, *Genome Res.*, **20**, 110-121, https://doi.org/10.1101/gr.097857.109.
31. Abramson, J., Adler, J., Dunger, J., Evans, R., Green, T., Pritzel, A., Ronneberger, O., Willmore, L., Ballard, A. J., Bambrick, J., Bodenstein, S. W., Evans, D. A., Hung, C. C., O'Neill, M., Reiman, D., Tunyasuvunakool, K., Wu, Z., Zemgulyte, A., Arvaniti, E., Beattie, C., et al. (2024) Accurate structure prediction of biomolecular interactions with AlphaFold 3, *Nature*, **630**, 493-500, https://doi.org/10.1038/s41586-024-07487-w.
32. Thompson, J. D., Higgins, D. G., and Gibson, T. J. (1994) CLUSTAL W: improving the sensitivity of progressive multiple sequence alignment through sequence weighting, position-specific gap penalties and weight matrix choice, *Nucleic Acids Res.*, **22**, 4673-4680, https://doi.org/10.1093/nar/22.22.4673.
33. Boulon, S., Marmier-Gourrier, N., Pradet-Balade, B., Wurth, L., Verheggen, C., Jady, B. E., Rothe, B., Pescia, C., Robert, M. C., Kiss, T., Bardoni, B., Krol, A., Branlant, C., Allmang, C., Bertrand, E., and Charpentier, B. (2008) The Hsp90 chaperone controls the biogenesis of L7Ae RNPs through conserved machinery, *J. Cell Biol.*, **180**, 579-595, https://doi.org/10.1083/jcb.200708110.
34. Cloutier, P., Poitras, C., Durand, M., Hekmat, O., Fiola-Masson, E., Bouchard, A., Faubert, D., Chabot, B., and Coulombe, B. (2017) R2TP/Prefoldin-like component RUVBL1/RUVBL2 directly interacts with ZNHIT2 to regulate assembly of U5 small nuclear ribonucleoprotein, *Nat. Commun.*, **8**, 15615, https://doi.org/10.1038/ncomms15615.
35. Malinova, A., Cvackova, Z., Mateju, D., Horejsi, Z., Abeza, C., Vandermoere, F., Bertrand, E., Stanek, D., and Verheggen, C. (2017) Assembly of the U5 snRNP component PRPF8 is controlled by the HSP90/R2TP chaperones, *J. Cell Biol.*, **216**, 1579-1596, https://doi.org/10.1083/jcb.201701165.
36. Horejsi, Z., Takai, H., Adelman, C. A., Collis, S. J., Flynn, H., Maslen, S., Skehel, J. M., de Lange, T., and Boulton, S. J. (2010) CK2 phospho-dependent binding of R2TP complex to TEL2 is essential for mTOR and SMG1 stability, *Mol. Cell*, **39**, 839-850, https://doi.org/10.1016/j.molcel.2010.08.037.
37. Kim, S. G., Hoffman, G. R., Poulogiannis, G., Buel, G. R., Jang, Y. J., Lee, K. W., Kim, B. Y., Erikson, R. L., Cantley, L. C., Choo, A. Y., and Blenis, J. (2013) Metabolic stress controls mTORC1 lysosomal localization and dimerization by regulating the TTT-RUVBL1/2 complex, *Mol. Cell*, **49**, 172-185, https://doi.org/10.1016/j.molcel.2012.10.003.
38. Boulon, S., Pradet-Balade, B., Verheggen, C., Molle, D., Boireau, S., Georgieva, M., Azzag, K., Robert, M. C., Ahmad, Y., Neel, H., Lamond, A. I., and Bertrand, E. (2010) HSP90 and its R2TP/Prefoldin-like cochaperone are involved in the cytoplasmic assembly of RNA polymerase II, *Mol. Cell*, **39**, 912-924, https://doi.org/10.1016/j.molcel.2010.08.023.
39. Nelde, A., Flototto, L., Jurgens, L., Szymik, L., Hubert, E., Bauer, J., Schliemann, C., Kessler, T., Lenz, G., Rammensee, H. G., Walz, J. S., and Wethmar, K. (2022) Upstream open reading frames regulate translation

of cancer-associated transcripts and encode HLA-presented immunogenic tumor antigens, *Cell. Mol. Life Sci.*, **79**, 171, https://doi.org/10.1007/s00018-022-04145-0.

40. Noderer, W. L., Flockhart, R. J., Bhaduri, A., Diaz de Arce, A. J., Zhang, J., Khavari, P. A., and Wang, C. L. (2014) Quantitative analysis of mammalian translation initiation sites by FACS-seq, *Mol. Systems Biol.*, **10**, 748, https://doi.org/10.15252/msb.20145136.
41. Andreev, D. E., O'Connor, P. B., Fahey, C., Kenny, E. M., Terenin, I. M., Dmitriev, S. E., Cormican, P., Morris, D. W., Shatsky, I. N., and Baranov, P. V. (2015) Translation of 5′ leaders is pervasive in genes resistant to eIF2 repression, *eLife*, **4**, e03971, https://doi.org/10.7554/eLife.03971.
42. Rocha, A. L., Pai, V., Perkins, G., Chang, T., Ma, J., De Souza, E. V., Chu, Q., Vaughan, J. M., Diedrich, J. K., Ellisman, M. H., and Saghatelian, A. (2024) An inner mitochondrial membrane microprotein from the SLC35A4 upstream ORF regulates cellular metabolism, *J. Mol. Biol.*, **436**, 168559, https://doi.org/10.1016/j.jmb.2024.168559.
43. Yang, H., Li, Q., Stroup, E. K., Wang, S., and Ji, Z. (2024) Widespread stable noncanonical peptides identified by integrated analyses of ribosome profiling and ORF features, *Nat. Commun.*, **15**, 1932, https://doi.org/10.1038/s41467-024-46240-9.
44. Ury, B., Potelle, S., Caligiore, F., Whorton, M. R., and Bommer, G. T. (2021) The promiscuous binding pocket of SLC35A1 ensures redundant transport of CDP-ribitol to the Golgi, *J. Biol. Chem.*, **296**, 100789, https://doi.org/10.1016/j.jbc.2021.100789.
45. Gerin, I., Ury, B., Breloy, I., Bouchet-Seraphin, C., Bolsee, J., Halbout, M., Graff, J., Vertommen, D., Muccioli, G. G., Seta, N., Cuisset, J. M., Dabaj, I., Quijano-Roy, S., Grahn, A., Van Schaftingen, E., and Bommer, G. T. (2016) ISPD produces CDP-ribitol used by FKTN and FKRP to transfer ribitol phosphate onto alpha-dystroglycan, *Nat. Commun.*, **7**, 11534, https://doi.org/10.1038/ncomms11534.
46. Sidrauski, C., McGeachy, A. M., Ingolia, N. T., and Walter, P. (2015) The small molecule ISRIB reverses the effects of eIF2alpha phosphorylation on translation and stress granule assembly, *eLife*, **4**, e05033, https://doi.org/10.7554/eLife.05033.
47. Palmer, C. S., Osellame, L. D., Laine, D., Koutsopoulos, O. S., Frazier, A. E., and Ryan, M. T. (2011) MiD49 and MiD51, new components of the mitochondrial fission machinery, *EMBO Rep.*, **12**, 565-573, https://doi.org/10.1038/embor.2011.54.
48. Yu, R., Liu, T., Jin, S. B., Ankarcrona, M., Lendahl, U., Nister, M., and Zhao, J. (2021) MIEF1/2 orchestrate mitochondrial dynamics through direct engagement with both the fission and fusion machineries, *BMC Biol.*, **19**, 229, https://doi.org/10.1186/s12915-021-01161-7.
49. Brown, A., Rathore, S., Kimanius, D., Aibara, S., Bai, X. C., Rorbach, J., Amunts, A., and Ramakrishnan, V. (2017) Structures of the human mitochondrial ribosome in native states of assembly, *Nat. Struct. Mol. Biol.*, **24**, 866-869, https://doi.org/10.1038/nsmb.3464.
50. Rathore, A., Chu, Q., Tan, D., Martinez, T. F., Donaldson, C. J., Diedrich, J. K., Yates, J. R., 3rd, and Saghatelian, A. (2018) MIEF1 microprotein regulates mitochondrial translation, *Biochemistry*, **57**, 5564-5575, https://doi.org/10.1021/acs.biochem.8b00726.
51. Chen, J., Brunner, A. D., Cogan, J. Z., Nunez, J. K., Fields, A. P., Adamson, B., Itzhak, D. N., Li, J. Y., Mann, M., Leonetti, M. D., and Weissman, J. S. (2020) Pervasive functional translation of noncanonical human open reading frames, *Science*, **367**, 1140-1146, https://doi.org/10.1126/science.aay0262.
52. Delcourt, V., Brunelle, M., Roy, A. V., Jacques, J. F., Salzet, M., Fournier, I., and Roucou, X. (2018) The protein coded by a short open reading frame, not by the annotated coding sequence, is the main gene product of the dual-coding gene MIEF1, *Mol. Cell. Proteomics*, **17**, 2402-2411, https://doi.org/10.1074/mcp.RA118.000593.
53. Grosely, R., Alvarado, C., Ivanov, I. P., Nicholson, O. B., Puglisi, J. D., Dever, T. E., and Lapointe, C. P. (2024) eIF1 and eIF5 dynamically control translation start site fidelity, *bioRxiv*, https://doi.org/10.1101/2024.07.10.602410.
54. Ly, J., Xiang, K., Su, K. C., Sissoko, G. B., Bartel, D. P., and Cheeseman, I. M. (2024) Nuclear release of eIF1 globally increases stringency of start-codon selection to preserve mitotic arrest physiology, *bioRxiv*, https://doi.org/10.1101/2024.04.06.588385.
55. Loughran, G., Sachs, M. S., Atkins, J. F., and Ivanov, I. P. (2012) Stringency of start codon selection modulates autoregulation of translation initiation factor eIF5, *Nucleic Acids Res.*, **40**, 2898-2906, https://doi.org/10.1093/nar/gkr1192.
56. Ivanov, I. P., Loughran, G., Sachs, M. S., and Atkins, J. F. (2010) Initiation context modulates autoregulation of eukaryotic translation initiation factor 1 (eIF1), *Proc. Natl. Acad. Sci. USA*, **107**, 18056-18060, https://doi.org/10.1073/pnas.1009269107.
57. Llacer, J. L., Hussain, T., Saini, A. K., Nanda, J. S., Kaur, S., Gordiyenko, Y., Kumar, R., Hinnebusch, A. G., Lorsch, J. R., and Ramakrishnan, V. (2018) Translational initiation factor eIF5 replaces eIF1 on the 40S ribosomal subunit to promote start-codon recognition, *eLife*, 7, e39273, https://doi.org/10.7554/eLife.39273.
58. Martin-Marcos, P., Cheung, Y. N., and Hinnebusch, A. G. (2011) Functional elements in initiation factors 1, 1A, and 2beta discriminate against poor AUG context and non-AUG start codons, *Mol. Cell. Biol.*, **31**, 4814-4831, https://doi.org/10.1128/MCB.05819-11.
59. Nanda, J. S., Cheung, Y. N., Takacs, J. E., Martin-Marcos, P., Saini, A. K., Hinnebusch, A. G., and

Lorsch, J. R. (2009) eIF1 controls multiple steps in start codon recognition during eukaryotic translation initiation, *J. Mol. Biol.*, **394**, 268-285, https://doi.org/10.1016/j.jmb.2009.09.017.

60. Hacisuleyman, E., Hale, C. R., Noble, N., Luo, J. D., Fak, J. J., Saito, M., Chen, J., Weissman, J. S., and Darnell, R. B. (2024) Neuronal activity rapidly reprograms dendritic translation via eIF4G2:uORF binding, *Nat. Neurosci.*, **27**, 822-835, https://doi.org/10.1038/s41593-024-01615-5.
61. Shestakova, E. D., Tumbinsky, R. S., Andreev, D. E., Rozov, F. N., Shatsky, I. N., and Terenin, I. M. (2023) The roles of eIF4G2 in leaky scanning and reinitiation on the human dual-coding POLG mRNA, *Int. J. Mol. Sci.*, **24**, 17149, https://doi.org/10.3390/ijms242417149.
62. She, R., Luo, J., and Weissman, J. S. (2023) Translational fidelity screens in mammalian cells reveal eIF3 and eIF4G2 as regulators of start codon selectivity, *Nucleic Acids Res.*, **51**, 6355-6369, https://doi.org/10.1093/nar/gkad329.
63. Weber, R., Kleemann, L., Hirschberg, I., Chung, M. Y., Valkov, E., and Igreja, C. (2022) DAP5 enables main ORF translation on mRNAs with structured and uORF-containing 5′ leaders, *Nat. Commun.*, **13**, 7510, https://doi.org/10.1038/s41467-022-35019-5.
64. David, M., Olender, T., Mizrahi, O., Weingarten-Gabbay, S., Friedlander, G., Meril, S., Goldberg, N., Savidor, A., Levin, Y., Salomon, V., Stern-Ginossar, N., Bialik, S., and Kimchi, A. (2022) DAP5 drives translation of specific mRNA targets with upstream ORFs in human embryonic stem cells, *RNA*, **28**, 1325-1336, https://doi.org/10.1261/rna.079194.122.
65. Smirnova, V. V., Shestakova, E. D., Nogina, D. S., Mishchenko, P. A., Prikazchikova, T. A., Zatsepin, T. S., Kulakovskiy, I. V., Shatsky, I. N., and Terenin, I. M. (2022) Ribosomal leaky scanning through a translated uORF requires eIF4G2, *Nucleic Acids Res.*, **50**, 1111-1127, https://doi.org/10.1093/nar/gkab1286.
66. Loughran, G., Zhdanov, A. V., Mikhaylova, M. S., Rozov, F. N., Datskevich, P. N., Kovalchuk, S. I., Serebryakova, M. V., Kiniry, S. J., Michel, A. M., O'Connor, P. B. F., Papkovsky, D. B., Atkins, J. F., Baranov, P. V., Shatsky, I. N., and Andreev, D. E. (2020) Unusually efficient CUG initiation of an overlapping reading frame in POLG mRNA yields novel protein POLGARF, *Proc. Natl. Acad. Sci. USA*, **117**, 24936-24946, https://doi.org/10.1073/pnas.2001433117.
67. Mudge, J. M., Ruiz-Orera, J., Prensner, J. R., Brunet, M. A., Calvet, F., Jungreis, I., Gonzalez, J. M., Magrane, M., Martinez, T. F., Schulz, J. F., Yang, Y. T., Alba, M. M., Aspden, J. L., Baranov, P. V., Bazzini, A. A., Bruford, E., Martin, M. J., Calviello, L., Carvunis, A. R., Chen, J., et al. (2022) Standardized annotation of translated open reading frames, *Nat. Biotechnol.*, **40**, 994-999, https://doi.org/10.1038/s41587-022-01369-0.